Template-Directed Synthesis of a Conjugated Zinc Porphyrin Nanoball

Jonathan Cremers,[†] Renée Haver,[†] Michel Rickhaus,[†] Juliane Q. Gong,[‡] Ludovic Favereau,[†] Martin D. Peeks,[†] Tim D. W. Claridge,[†] Laura M. Herz,[‡] and Harry L. Anderson*,[†]

[†]Chemistry Research Laboratory, Department of Chemistry, University of Oxford, Oxford OX1 3TA, United Kingdom
[‡]Clarendon Laboratory, Department of Physics, University of Oxford, Oxford OX1 3PU, United Kingdom

S *Supporting Information*

ABSTRACT: We report the template-directed synthesis of a π-conjugated 14-porphyrin nanoball. This structure consists of two intersecting nanorings containing six and 10 porphyrin units. Fluorescence upconversion spectroscopy experiments demonstrate that electronic excitation delocalizes over the whole three-dimensional π system in less than 0.3 ps if the nanoball is bound to its templates or over 2 ps if the nanoball is empty.

Spurred by the discovery of buckminsterfullerene,[1] chemists have sought rational strategies for the synthesis of three-dimensional (3D) π-conjugated geodesic cages. Stepwise chemical synthesis has not yet been used to prepare any fullerenes except C_{60} (ref 2), but several fullerene-like ball-shaped π-conjugated hydrocarbons have been synthesized recently.[3] The high dimensionality of these π systems is expected to enhance their electronic delocalization compared with 1D or 2D molecular semiconductors.[4−6] Shape-persistent molecular cages are also in demand for their gas adsorption properties, which mimic those of zeolites.[7] The best routes to molecular cages or capsules use reversible reactions that allow error correction, such as metal coordination[8] or boronic ester condensation,[9] but these reactions do not produce π-conjugated connections. In principle, reversible reactions such as imine formation,[10] alkene metathesis,[11] and alkyne metathesis[12] could be used to construct π-conjugated cages, but to date the cages made by these reactions lack long-range conjugation.[7,10−12] Template-directed coupling under kinetic control is an alternative strategy for preparing large macrocycles and cages.[13] Here we show how simple molecular templates can be used to synthesize the first fully π-conjugated porphyrin ball, *b*-P14 (Figure 1). This 14-porphyrin prolate-ellipsoidal cage consists of two perpendicular intersecting conjugation pathways, one containing six and the other 10 porphyrin units. Structures of this type are valuable models for photosynthetic light-harvesting systems.[13−15] When all 14 porphyrin units in *b*-P14 are bound to templates, locking the conformation, excited-state energy delocalization occurs over the whole system within 0.3 ps, whereas in the absence of the templates excitation is distributed over the ball with a time constant of about 2 ps.

The porphyrin nanoball *b*-P14 was synthesized as shown in Figure 2 using templates T6 and T4 (Figure 1). This route starts from a six-porphyrin nanoring template complex with four terminal alkyne substituents, *c*-P6(H)4·T6, which was prepared
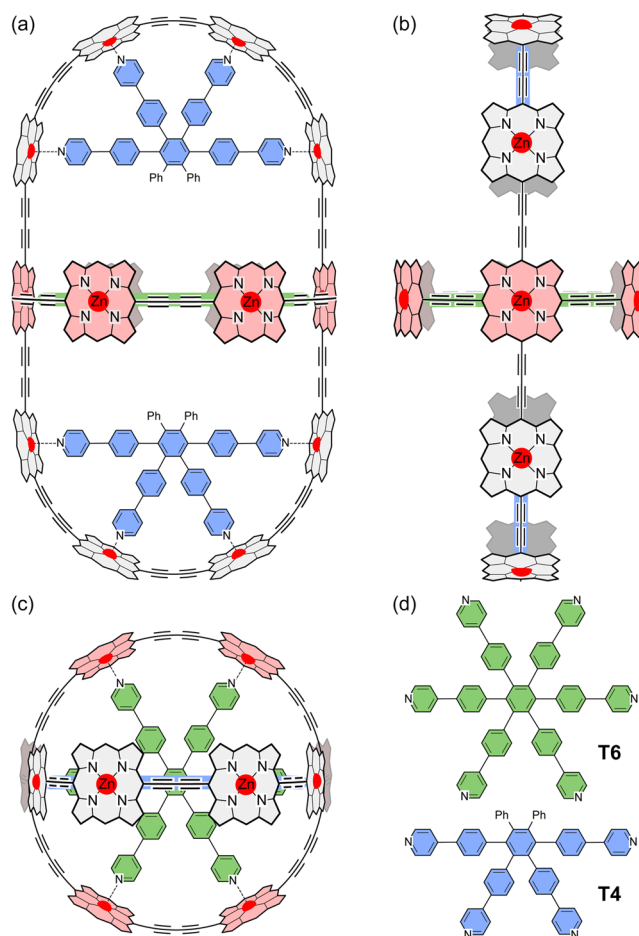

Figure 1. (a−c) Three orthogonal views of the structure of the 14-porphyrin ball template complex *b*-P14·T6·(T4)2 and (d) structures of the templates T6 and T4. The *meso*-aryl side groups on the porphyrins have been omitted for clarity.

as reported previously.[16] This ring was coupled to four porphyrin dimers, P2-CPDIPS, followed by removal of the CPDIPS protecting groups, to give the extended nanoring *c*-P6(P2)4·T6. The four-legged template T4 was then used to close the 10-porphyrin ring, yielding the bicyclic nanoball *b*-P14·T6·(T4)2.
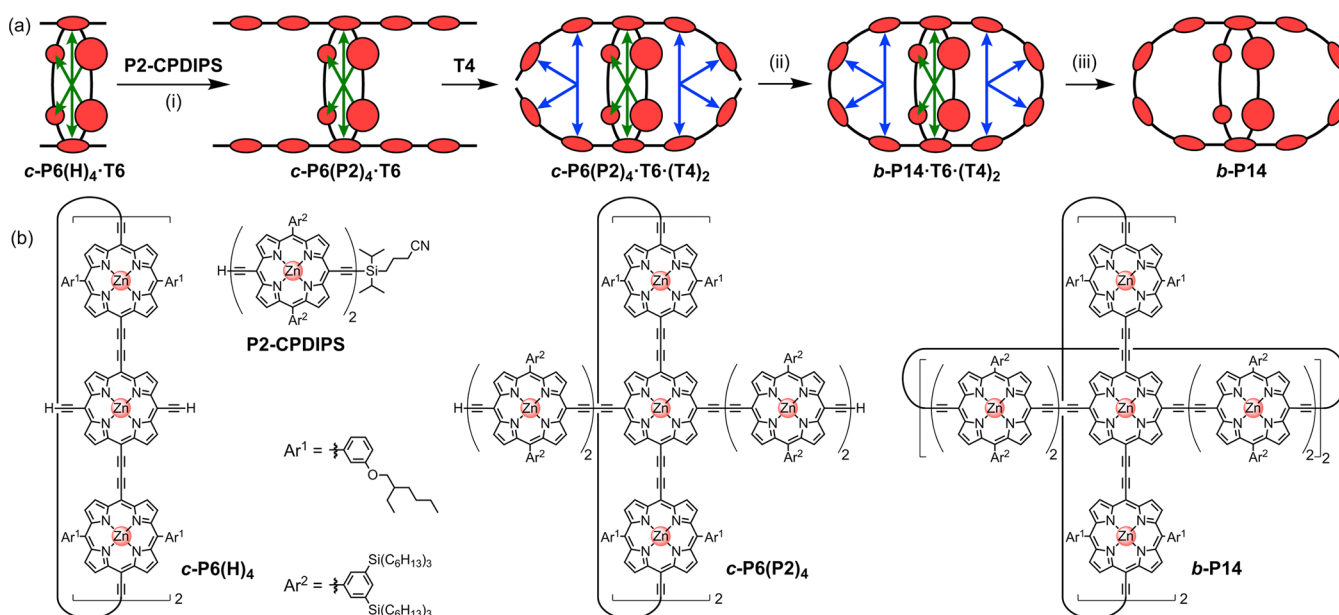
Figure 2. (a) Schematic synthetic route for **b-P14**. Reaction conditions: (i) **P2-CPDIPS**, Pd(PPh$_3$)$_2$Cl$_2$, CuI, 1,4-benzoquinone, CHCl$_3$/*i*-Pr$_2$NH, 41%; then TBAF, CH$_2$Cl$_2$, 97%; (ii) Pd(PPh$_3$)$_2$Cl$_2$, CuI, 1,4-benzoquinone, CHCl$_3$/*i*-Pr$_2$NH, 51%; (iii) DABCO, size-exclusion chromatography, toluene/pyridine, 100%. (b) Chemical structures of **c-P6(H)$_4$**, **P2-CPDIPS**, **c-P6(P2)$_4$**, and **b-P14**.

The templates can readily be displaced from this cage by high concentrations of a competing ligand;[17] quinuclidine or 1,4-diazabicyclo[2.2.2]octane (DABCO) removes both templates, giving **b-P14**, whereas pyridine selectively removes **T4**, giving **b-P14·T6**. Both **b-P14** and **b-P14·T6** were fully characterized (see the Supporting Information). Two types of aryl solubilizing groups were used in this molecular design (Ar^1 and Ar^2; Figure 2) to confer high solubility while avoiding excessive steric congestion.

Gel-permeation chromatography (GPC) confirmed the purity of the nanoball and showed that its molecular weight is in the expected range (ca. 20 kDa). The ^{1}H NMR spectrum of **b-P14·T6·(T4)$_2$** in CDCl$_3$ at 298 K is consistent with the expected D_{2h} gross symmetry, and all of the signals were assigned by NMR correlation spectroscopy and nuclear Overhauser effect spectroscopy, except for unresolved aliphatic multiplets in the 0.4–2.0 ppm region (see the Supporting Information). The ^{1}H NMR spectrum shows that the nanoball consists of a mixture of conformers with ethylhexyl chains pointing into and out of the cavity; these rotamers are in slow exchange on the NMR time scale, with ca. 40% of the alkoxy chains pointing toward the center of the ball. This ratio scarcely changes upon removal of the **T4** templates. When all of the templates are removed, the porphyrins of the six-porphyrin ring rotate rapidly, simplifying the NMR spectrum. Diffusion-ordered ^{1}H NMR spectroscopy experiments show that **b-P14·T6·(T4)$_2$** has a diffusion coefficient of 1.52×10^{-10} m^2 s^{-1} (700 MHz, 298 K, CDCl$_3$), which corresponds to an effective hydrodynamic radius of 27 Å, calculated using the Stokes–Einstein equation for a spherical molecule.

The UV–vis–NIR spectrum of **b-P14·T6·(T4)$_2$** (Figure 3a, black curve) is essentially the sum of the absorption spectra of its two component rings, as modeled by **c-P6·T6** (the D_{6h} ring complex with 3,5-bis(trihexylsilyl)phenyl substituents)[18] and **c-P10·(T5)$_2$** (where **T5** is the version of **T6** with five pyridyl sites),[16–20] although the absorption spectrum of **b-P14·T6·(T4)$_2$** is slightly red-shifted, demonstrating greater π conjugation (Figure S82). When **b-P14·T6·(T4)$_2$** is treated with quinuclidine
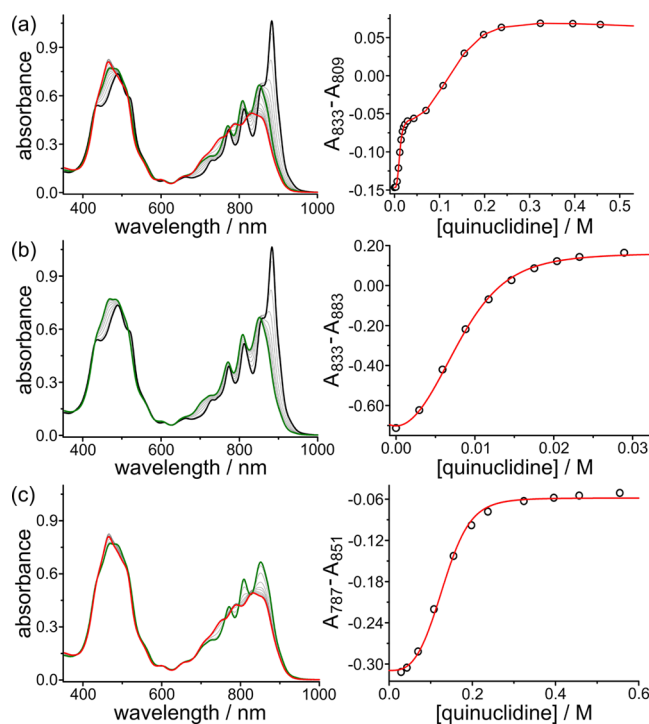

Figure 3. UV–vis–NIR denaturation titration of the **b-P14·T6·(T4)$_2$** complex with quinuclidine (toluene, 298 K). (a) Full titration, in which **T4** is displaced first (black to green), followed by the displacement of **T6** (green to red). The two phases of the titration are shown in (b) and (c), with the experimental (black circles) and calculated (red lines) isotherms shown on the right.

to displace the templates, two distinct denaturation processes are observed in the UV–vis–NIR titration (Figure 3): At quinuclidine concentrations of 3–30 mM (Figure 3b), the **T4** units are displaced, leading to disappearance of the sharp peak at 883 nm;[19–21] this peak is associated with the template-bound conformation of the 10-porphyrin ring. At quinuclidine

concentrations of 30−300 mM (Figure 3c), the central **T6** unit is displaced, causing disappearance of the distinctive three-finger pattern in the Q band of the six-porphyrin ring component. All of these spectral changes reflect the greater flexibility and wider distribution of porphyrin−porphyrin dihedral angles upon template removal.

Analysis of the denaturation binding isotherms[13c,17,21] (Figure 3) reveals that the association constants for binding of **T4** and **T6** to **b-P14** to form **b-P14·T6·(T4)₂** are $(1.8 \pm 0.2) \times 10^{22}$ M^{-1} for **T4** and $(5.5 \pm 1.2) \times 10^{37}$ M^{-1} for **T6** in toluene at 298 K. This analysis assumes that the denaturation processes for the two templates (**T4** and **T6**) are essentially all-or-nothing two-state equilibria (i.e., intermediate partially denatured species do not build up to high concentrations); this assumption is supported by the isosbestic nature of the UV−vis−NIR titration and the good fits of the curves to the calculated isotherm for a two-state equilibrium (Figure 3b,c). The binding strength of **T6** is roughly an order of magnitude stronger in the ball than in a comparable six-ring system,[17] which can be attributed to the conformational preorganization provided by the 10-porphyrin ring.

The UV−vis−NIR absorption and fluorescence spectra of **b-P14·T6·(T4)₂** and **b-P14** are compared in Figure 4. The more
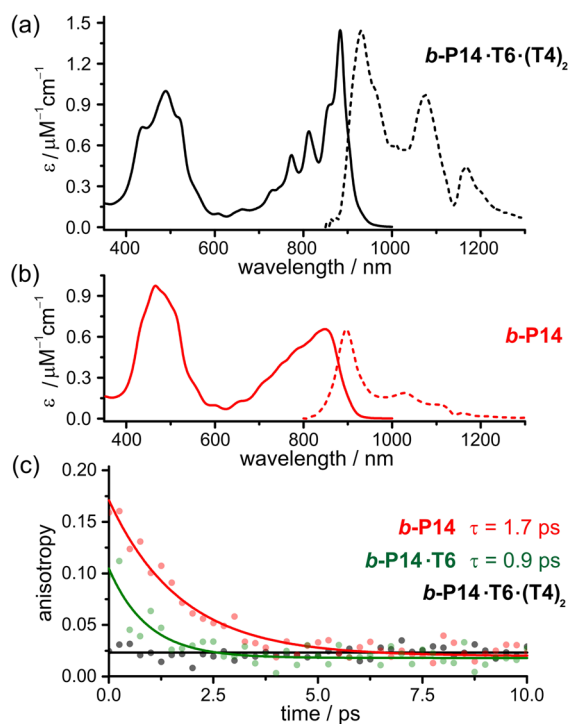

Figure 4. UV−vis−NIR absorption (solid lines) and fluorescence (dashed lines) spectra of (a) **b-P14·T6·(T4)₂** and (b) **b-P14** (toluene, 298 K). The dip at 1130−1170 nm corresponds to solvent absorption. (c) First-order fits of the fluorescence anisotropy decay. Solutions of **b-P14·T6·(T4)₂** (black), **b-P14·T6** (green), and **b-P14** (red) were excited at 820 nm, and emission was detected at 950 nm.

rigid conformation of the template-bound ball is reflected by its sharper and more red-shifted absorption and emission spectra.[19−21] Fluorescence upconversion spectroscopy experiments reveal that the excited states delocalize across the two perpendicular ring planes in the nanoball on an ultrashort time scale. The fluorescence anisotropy dynamics of **b-P14** with and without templates are shown in Figure 4c. The template complex, **b-P14·T6·(T4)₂** (black points), exhibits a constant

and very low anisotropy ($\gamma = 0.02$) over the time range of this experiment (0−10 ps; time resolution = 0.3 ps), showing that the excited state delocalizes in three dimensions within 0.3 ps. In contrast, **b-P14·T6** (green points) and **b-P14** (red points) show a fast initial drop in anisotropy within the first 5 ps from $\gamma = 0.1$ toward $\gamma \approx 0$. This fast depolarization resembles the anisotropy decay in porphyrin nanorings with >24 porphyrin units.[15] The initial anisotropy of 0.1 suggests that upon excitation, an exciton is delocalized over a full ring and that both absorption and emission transition dipoles are polarized in the ring plane. After ultrafast relaxation, the exciton localizes and migrates rapidly around the entire porphyrin nanoball. Contributions from emission components polarized in both planes thus result in an anisotropy close to zero. Without the templates, exciton migration is slower, resulting in the observed anisotropy decays, whereas in **b-P14·T6·(T4)₂** the anisotropy decay is faster than the time resolution of the experiment. This behavior is very different from that of the nanorings **c-P6·T6**, **c-P6**, and **c-P10**, which exhibit anisotropies of near 0.1 (remaining constant during 10 ps after excitation), in agreement with theoretical predictions for an excited state that is delocalized over a 2D ring.[15,16,18,20,22]

The prolate shape of **b-P14·T6·(T4)₂** and **b-P14** is reminiscent of C_{70} fullerene. While C_{60} fullerene has complete polarization memory loss with zero fluorescence anisotropy, C_{70} displays excitation-wavelength-dependent anisotropy values ranging between −0.2 and 0.1 because emission polarized in the xy plane is energetically favorable as a result of geometrical deformation.[23] However, **b-P14·T6·(T4)₂** and **b-P14** do not display any significant changes in anisotropy with excitation wavelength in the range of 760−880 nm, probably because the absorption features of their two constituent rings broadly overlap and the emission may be polarized in both ring planes. Density functional theory (DFT) calculations (B3LYP/6-31G*) indicate that the HOMO of **b-P14** is distributed over the entire π system (Figure 5), albeit with a higher density on the six-porphyrin ring and particularly the tetraalkynylporphyrins. The LUMO and LUMO+1 are located exclusively on the six-porphyrin ring and
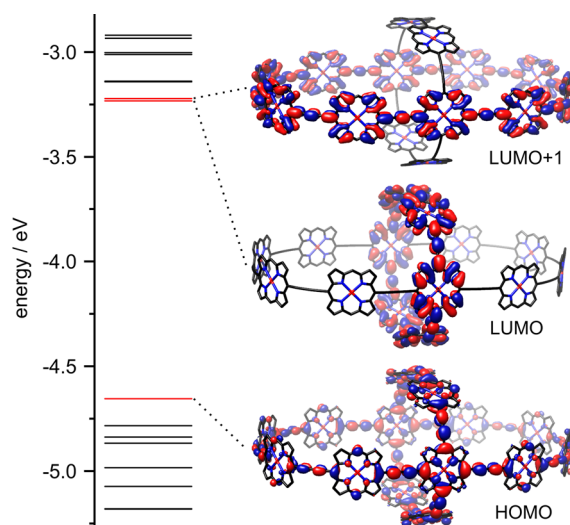

Figure 5. LUMO+1 (−3.22 eV), LUMO (−3.23 eV), and HOMO (−4.66 eV) of **b-P14** calculated at the B3LYP/6-31G* level of theory with Grimme's dispersion correction (GD3), shown at a density isovalue of 0.008 au together with their corresponding energy levels. Aryl groups were replaced with hydrogen atoms to simplify the calculations.

the 10-porphyrin ring, respectively, with nearly identical energies. Time-dependent DFT calculations (B3LYP/6-31G*) were carried out to model the electronic excited states of **b-P14**. Natural transition orbital plots (Tables S5−S13) show that the two lowest-energy singlet excited states (S_1 and S_2) are mainly localized in the six-porphyrin and 10-porphyrin ring components, respectively. The $S_0 \rightarrow S_1$ and $S_0 \rightarrow S_2$ transitions are dipole-forbidden ($f = 0$), whereas transitions to S_3, S_4, and S_5 are allowed ($f = 0.13$, 5.12, and 0.83, respectively), and these excited states are distributed over all 14 porphyrins. These calculations are in line with the observation that excitation delocalizes between the two rings within the ball on a time scale of less than 300 fs. The dimensions of the calculated geometry of **b-P14** are 52.7, 27.6, and 23.9 Å (measured as the diameter along the D_{2h} symmetry axes, without including aryl side chains).

In summary, we have synthesized a fully π-conjugated three-dimensional 14-porphyrin nanoball by a template-directed approach. UV−vis−NIR titrations show that the templates bound within the cavity can be removed successively by the addition of a competing ligand. Fluorescence upconversion spectroscopy reveals ultrafast electronic delocalization between the two perpendicular ring planes in the porphyrin ball. The fluorescence anisotropy approaches zero, indicating that excitation rapidly migrates between the two ring components of the nanoball.

■ ASSOCIATED CONTENT

Ⓢ Supporting Information

The Supporting Information is available free of charge on the ACS Publications website at DOI: 10.1021/jacs.8b02552.

> Synthetic procedures, characterization data, binding studies, NMR assignments, fluorescence spectroscopy, and calculated geometries (PDF)
> Coordinate file (XYZ)

■ AUTHOR INFORMATION

Corresponding Author
*harry.anderson@chem.ox.ac.uk

ORCID Ⓞ
Michel Rickhaus: 0000-0002-6107-2310
Martin D. Peeks: 0000-0002-9057-9444
Tim D. W. Claridge: 0000-0001-5583-6460
Laura M. Herz: 0000-0001-9621-334X
Harry L. Anderson: 0000-0002-1801-8132

Notes
The authors declare no competing financial interest.

■ ACKNOWLEDGMENTS

■ REFERENCES

(1) Kroto, H. W.; Heath, J. R.; O'Brien, S. C.; Curl, R. F.; Smalley, R. E. *Nature* **1985**, *318*, 162.
(2) (a) Scott, L. T.; Boorum, M. M.; McMahon, B. J.; Hagen, S.; Mack, J.; Blank, J.; Wegner, H.; de Meijere, A. *Science* **2002**, *295*, 1500. (b) Kabdulov, M.; Jansen, M.; Amsharov, K. Yu *Chem. - Eur. J.* **2013**, *19*, 17262. (c) Greisch, J.-F.; Amsharov, K. Yu.; Weippert, J.; Weis, P.; Böttcher, A.; Kappes, M. M. *J. Am. Chem. Soc.* **2016**, *138*, 11254.
(3) (a) Matsui, K.; Segawa, Y.; Namikawa, T.; Kamada, K.; Itami, K. *Chem. Sci.* **2013**, *4*, 84. (b) Kayahara, E.; Iwamoto, T.; Takaya, H.; Suzuki, T.; Fujitsuka, M.; Majima, T.; Yasuda, N.; Matsuyama, N.; Seki, S.; Yamago, S. *Nat. Commun.* **2013**, *4*, 2694. (c) Matsui, K.; Segawa, Y.; Itami, K. *J. Am. Chem. Soc.* **2014**, *136*, 16452. (d) Ikemoto, K.; Kobayashi, R.; Sato, S.; Isobe, H. *Angew. Chem., Int. Ed.* **2017**, *56*, 6511.
(4) Gutzler, R.; Perepichka, D. F. *J. Am. Chem. Soc.* **2013**, *135*, 16585.
(5) Peeks, M. D.; Tait, C. E.; Neuhaus, P.; Fischer, G. M.; Hoffmann, M.; Haver, R.; Cnossen, A.; Harmer, J. R.; Timmel, C. R.; Anderson, H. L. *J. Am. Chem. Soc.* **2017**, *139*, 10461.
(6) Ball, M.; Zhong, Y.; Fowler, B.; Zhang, B.; Li, P.; Etkin, G.; Paley, D. W.; Decatur, J.; Dalsania, A. K.; Li, H.; Xiao, S.; Ng, F.; Steigerwald, M. L.; Nuckolls, C. *J. Am. Chem. Soc.* **2016**, *138*, 12861.
(7) (a) Zhang, G.; Mastalerz, M. *Chem. Soc. Rev.* **2014**, *43*, 1934. (b) Hasell, T.; Cooper, A. I. *Nat. Rev. Mater.* **2016**, *1*, 16053. (c) Santolini, V.; Miklitz, M.; Berardo, E.; Jelfs, K. E. *Nanoscale* **2017**, *9*, 5280.
(8) (a) Olenyuk, B.; Levin, M. D.; Whiteford, J. A.; Shield, J. E.; Stang, P. J. *J. Am. Chem. Soc.* **1999**, *121*, 10434. (b) Sun, Q.-F.; Iwasa, J.; Ogawa, D.; Ishido, Y.; Sato, S.; Ozeki, T.; Sei, Y.; Yamaguchi, K.; Fujita, M. *Science* **2010**, *328*, 1144.
(9) Zhang, G.; Presly, O.; White, F.; Oppel, I. M.; Mastalerz, M. *Angew. Chem., Int. Ed.* **2014**, *53*, 5126.
(10) Rue, N. M.; Sun, J.; Warmuth, R. *Isr. J. Chem.* **2011**, *51*, 743.
(11) Zhu, B.; Chen, H.; Lin, W.; Ye, Y.; Wu, J.; Li, S. *J. Am. Chem. Soc.* **2014**, *136*, 15126.
(12) (a) Zhang, C.; Wang, Q.; Long, H.; Zhang, W. *J. Am. Chem. Soc.* **2011**, *133*, 20995. (b) Lee, S.; Yang, A.; Moneypenny, T. P., II; Moore, J. S. *J. Am. Chem. Soc.* **2016**, *138*, 2182.
(13) (a) O'Sullivan, M. C.; Sprafke, J. K.; Kondratuk, D. V.; Rinfray, C.; Claridge, T. D.; Saywell, A.; Blunt, M. O.; O'Shea, J. N.; Beton, P. H.; Malfois, M.; Anderson, H. L. *Nature* **2011**, *469*, 72. (b) Neuhaus, P.; Cnossen, A.; Gong, J. Q.; Herz, L. M.; Anderson, H. L. *Angew. Chem., Int. Ed.* **2015**, *54*, 7344. (c) Favereau, L.; Cnossen, A.; Kelber, J. B.; Gong, J. Q.; Oetterli, R. M.; Cremers, J.; Herz, L. M.; Anderson, H. L. *J. Am. Chem. Soc.* **2015**, *137*, 14256.
(14) (a) Wasielewski, M. R. *Acc. Chem. Res.* **2009**, *42*, 1910. (b) Aratani, N.; Kim, D.; Osuka, A. *Acc. Chem. Res.* **2009**, *42*, 1922.
(15) Parkinson, P.; Kondratuk, D. V.; Menelaou, C.; Gong, J. Q.; Anderson, H. L.; Herz, L. M. *J. Phys. Chem. Lett.* **2014**, *5*, 4356.
(16) Gong, J. Q.; Favereau, L.; Anderson, H. L.; Herz, L. M. *J. Phys. Chem. Lett.* **2016**, *7*, 332.
(17) Hogben, H. J.; Sprafke, J. K.; Hoffmann, M.; Pawlicki, M.; Anderson, H. L. *J. Am. Chem. Soc.* **2011**, *133*, 20962.
(18) Sprafke, J. K.; Kondratuk, D. V.; Wykes, M.; Thompson, A. L.; Hoffmann, M.; Drevinskas, R.; Chen, W.-H.; Yong, C. K.; Kärnbratt, J.; Bullock, J. E.; Malfois, M.; Wasielewski, M. R.; Albinsson, B.; Herz, L. M.; Zigmantas, D.; Beljonne, D.; Anderson, H. L. *J. Am. Chem. Soc.* **2011**, *133*, 17262.
(19) Liu, S.; Kondratuk, D. V.; Rousseaux, S. A. L.; Gil-Ramírez, G.; O'Sullivan, M. C.; Cremers, J.; Claridge, T. D. W.; Anderson, H. L. *Angew. Chem., Int. Ed.* **2015**, *54*, 5355.
(20) Gong, J. Q.; Parkinson, P.; Kondratuk, D. V.; Gil-Ramírez, G.; Anderson, H. L.; Herz, L. M. *J. Phys. Chem. C* **2015**, *119*, 6414.
(21) Cremers, J.; Richert, S.; Kondratuk, D. V.; Claridge, T. D. W.; Timmel, C. R.; Anderson, H. L. *Chem. Sci.* **2016**, *7*, 6961.
(22) Yong, C.-K.; Parkinson, P.; Kondratuk, D. V.; Chen, W.-H.; Stannard, A.; Summerfield, A.; Sprafke, J. K.; O'Sullivan, M. C.; Beton, P. H.; Anderson, H. L.; Herz, L. M. *Chem. Sci.* **2015**, *6*, 181.
(23) Fedorov, A.; Berberan-Santos, M. N.; Lefèvre, J.-P.; Valeur, B. *Chem. Phys. Lett.* **1997**, *267*, 467.